Atmospheric Chemistry

DOI: 10.1002/ange.201200656

# Reactivity of Atmospherically Relevant Small Radicals at the Air–Water Interface**

*Marilia T. C. Martins-Costa, Josep M. Anglada, Joseph S. Francisco, and Manuel F. Ruiz-Lopez**

Aerosols and clouds play important roles in atmospheric chemistry,[1] but molecular details of the process are not yet completely understood, despite many investigations carried out in the last few years. On one hand, the uptake of a compound into an aerosol or a water droplet modifies its gas-phase concentration and chemical kinetics. On the other hand, the condensed phase allows for otherwise unfeasible processes to occur in the atmosphere, ionic reactions in aqueous environments being a prototypical example. Indeed, the chemistry of one of the most important atmospheric species, the hydroperoxyl radical $HO_2$, is thought to be highly influenced by these type of reactions.[2] $HO_2$ is acidic ($pK_a$ 4.7) and can be efficiently scavenged by cloud droplets through the following processes:

$$HO_2(g) \rightleftharpoons HO_2(aq) \quad (1)$$

$$HO_2 \rightleftharpoons H^+ + O_2^- \quad (2)$$

$$HO_2 + O_2^- + H_2O \rightleftharpoons H_2O_2 + O_2 + OH^- \quad (3)$$

In parallel, a number of studies have provided evidence that chemistry in droplets and aerosols often involve heterogeneous reactions occurring at the surface. Though such processes still remain poorly understood, their impact on the global chemistry of the Earth's atmosphere is considered to be large, although further work is needed to quantitate the impact. As far as the interaction of $HO_2$ with water surfaces is concerned, several theoretical models and approaches have been employed.[3] Vácha et al.[3a] carried out molecular dynamics (MD) simulations at the air–water interface (they also considered other important atmospheric species, such as $N_2$, $O_2$, $O_3$, HO, and $H_2O_2$). A particular focus was the free-energy variation from the gas phase to the interface and the bulk. The interface–bulk partition is obviously a fundamental property in this context that is connected to the solvation free energy difference $\delta\Delta G_{solv} = \Delta G_{solv,interface} - \Delta G_{solv,bulk}$. Interestingly, $HO_2$ exhibited a global free energy minimum at the air–water interface with $\delta\Delta G_{solv} \approx -0.7$ kcal mol$^{-1}$. To the best of our knowledge, no equivalent simulations have been reported for $O_2^-$. Moreover, no studies have been devoted to analyze the electronic properties of these radicals (and hence their reactivity) at the air–water interface. The aim of this work is to shed light on these important questions that are crucial to better understand the role played by heterogeneous reactions in water droplets on the overall atmospheric chemistry.

Because we are interested on both free energy and electronic properties, we carried out MD simulations using a combined quantum/classical (QM/MM) force field[4] in which the solute is described quantum mechanically (QM) and the solvent is described using molecular mechanics (MM). We allow for electrostatic embedding, that is, the Hamiltonian of the solute includes the electrostatic interaction with solvent charges. We assumed the NVT ensemble ($T = 298$ K) using a box containing the radical ($HO_2$ or $O_2^-$) and 499 water molecules (TIP3P model[5]). Periodic boundary conditions are used along the $X$ and $Y$ directions. The radicals are described at the B3LYP/6-311+G* (for free energy calculations) or B3LYP/aug-cc-pVTZ levels[6] (for electronic properties calculations). The potential of mean force is computed using the umbrella sampling[7] and WHAM[8] methods. Other computational details are provided below. The stability of the radicals at the air–water interface is first verified by carrying out unconstrained MD simulations (50 ps) with the radicals initially placed at the interface. The results show that $HO_2$ remains at the interface all along the simulation, consistent with the results of Vácha et al.,[3a] while the calculation for $O_2^-$ shows, in contrast, a very fast migration of this species towards the bulk. The density profiles from these simulations are plotted in Figure 1.

First the results obtained for the free energy change between the bulk and the air–water interface will be discussed (Figure 2). In agreement with previous simulations, a shallow free energy minimum is predicted at the interface for $HO_2$ that is slightly below the bulk water free energy, $\delta\Delta G_{solv} \approx -0.5$ kcal mol$^{-1}$ (the experimental free energy of bulk solvation of $HO_2$ is about $-5$ kcal mol$^{-1}$[9]). In other words, the $HO_2$ radical exhibits a small but significant trend to accumulate at the interface. In the case of $O_2^-$, the free energy exhibits a continuous decrease from the interface to the bulk with $\delta\Delta G_{solv} \approx +5$ kcal mol$^{-1}$ (the experimental free energy of bulk solvation in water of the superoxide anion is $-85$ kcal mol$^{-1}$ [10]). Although this behavior is not unexpected for an ion, it contrasts with that found[11] for closely related systems such as $N_3^-$ and suggests that the superoxide anion is harder than assumed in some studies. It is interesting to note, however, that the free energy difference between the inter-

[*] Dr. M. T. C. Martins-Costa, Dr. M. F. Ruiz-Lopez
Equipe de Chimie et Biochimie Théoriques, SRSMC, CNRS, University of Lorraine
BP 70239, 54506 Vandoeuvre-les-Nancy (France)
E-mail: manuel.ruiz@uhp-nancy.fr
Dr. J. M. Anglada
Departament de Química Biològica i Modelització Molecular IQAC-CSIC, Barcelona (Spain)
Prof. J. S. Francisco
Department of Chemistry and Department of Earth and Atmospheric Science, Purdue University (USA)

[**] This work was supported by the French ANR (09-BLAN-0180-01) and the Spanish DGYCIT (CTQ2011-27812).

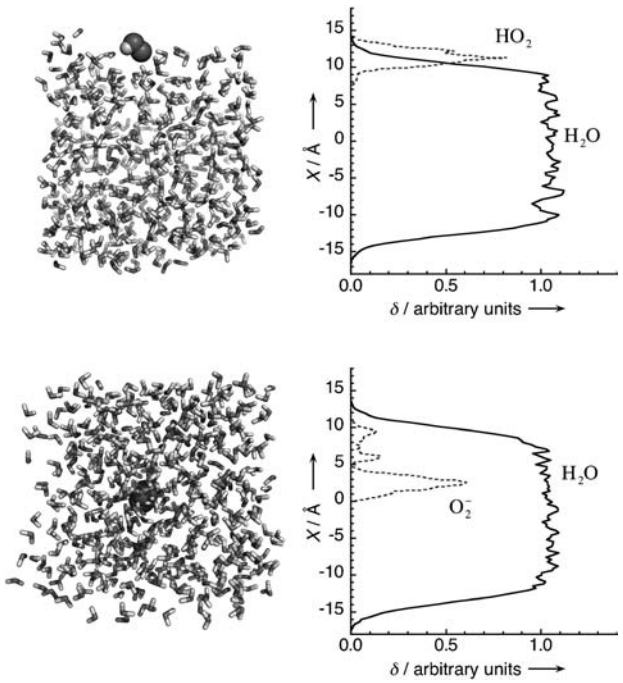


***Figure 1.*** Unconstrained 50 ps MD simulations with the radicals initially placed at the air–water interface. Left: Snapshots at the end of the simulation showing $HO_2$ at the air–water interface (upper) and $O_2^-$ in bulk water (lower). Right: Density profiles for the radicals and water ($X=0$ corresponds to the center of the simulation box).

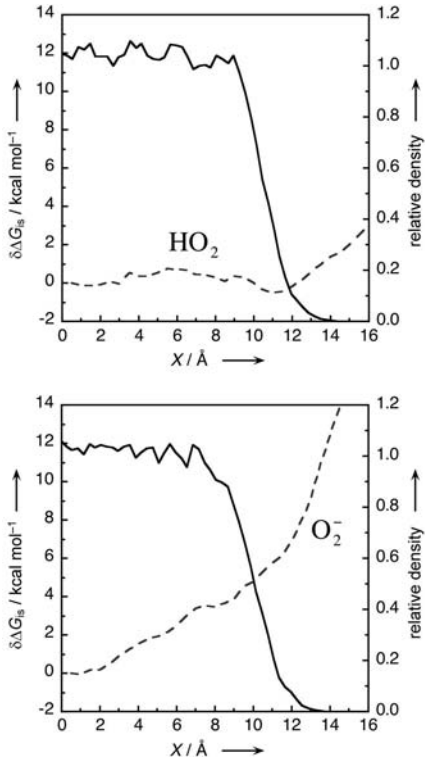


***Figure 2.*** Potential of mean force for $HO_2$ and $O_2^-$ radicals as a function of the distance to the air–water interface (-----). The water slab is indicated by the density of water (——). $X=0$ corresponds to the center of the simulation box.

face and the bulk is much smaller than the whole free energy of bulk solvation, suggesting that the radical is efficiently solvated upon reaching the interface.

The radial distribution functions (RDFs) at the interface and in the bulk are compared in Figure 3. They have been obtained from the unconstrained MD simulations in the bulk

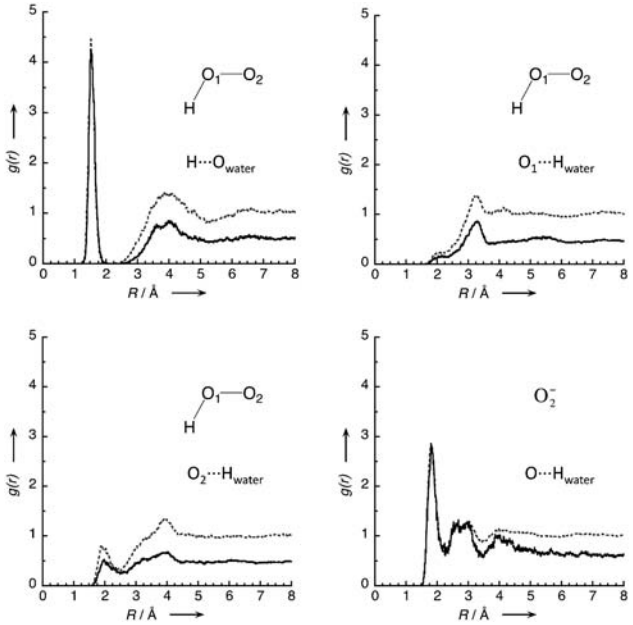


***Figure 3.*** Radial distribution functions $g(r)$ for hydrogen bonds between $HO_2$ or $O_2^-$ and water molecules. The results correspond to simulations with the radical at the interface (——) or in the bulk (-----). $R$ corresponds to the solute-solvent hydrogen-bond length. $O_{water}$ and $H_{water}$ hold for atoms in solvent water molecules.

or the interface; in the case of $O_2^-$, as the system is not stable at the interface, we have used the first 5 ps of the simulation (during which the anion remains at the interface). For $HO_2$, the RDFs show the formation of a strong hydrogen bond of the H-atom of the radical with water, with negligible differences between the interface and bulk solution for the first peak of the RDFs curves. Indeed, the integration of the peaks leads to hydration numbers of 1.0 in both cases. It should be noted that previous QM/MM simulations of the radical in bulk water[4c] showed that this species is a better proton donor than water but a poorer proton acceptor. The central O atom of the radical, as in bulk water, does not form significant H-bonds. The terminal O atom forms a weak H-bond with water and the RDF curves show that this H-bond is much less likely to form in the interface than in bulk water, the integrated hydration numbers being 0.20 and 0.74, respectively. The detailed analysis of the trajectory indicates that the radical spends a large part of the time in the air-side of the interface, with orientation favoring the interaction of its H atom with water molecules (Figure 4).

In the case of $O_2^-$, the results in the bulk are similar to previous AIMD simulations,[12] which pointed out some discrepancies with classical MD simulations for this system.[13] The first solvation shell at the interface and the

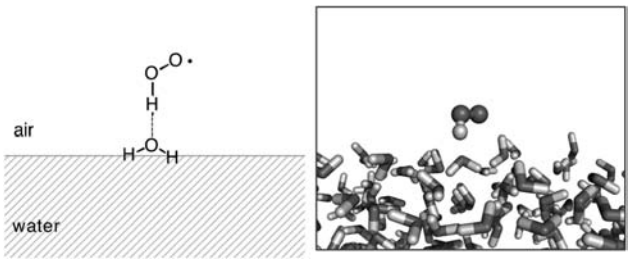


***Figure 4.*** Representation of the $HO_2$ radical stabilized at the air–water interface (left) and a snapshot from the QM/MM MD simulation (right).

bulk are quite similar and the hydration number is only slightly smaller at the interface. Integration of first peak leads to 1.62 (bulk) and 1.35 (interface) water molecules by oxygen atom, that is, to a total $O_2^-$ hydration number of 3.2 (bulk) and 2.7 (interface). The bulk calculation is not far from the experimental value 4.[14] It can be concluded that as the superoxide radical approaches the air–water interface in the uptake process, it rapidly completes its first solvation shell.

On the basis of the free energies presented above, a gradient of the relative concentrations $[HO_2]/[O_2^-]$ can be expected, with a larger concentration of the dissociated system in the bulk solvent and a smaller concentration at the interface. However, to estimate such concentrations, one needs to take into account the free energy of the proton. The affinity of the hydrated proton for the air–water interface was originally predicted computationally[15] and subsequently supported by additional experimental and computational research for acidic solutions.[16] The acidic or basic character of the neutral air–water interface has, however, been the subject of intense debate.[17] Very recent ab initio MD studies[16d] suggest a stabilization of $[H_3O^+]$ at the interface by as much as 3.6 kcal mol$^{-1}$ with respect to the bulk. Thus, a variation of the effective dissociation constant of $HO_2$ (that is, of the effective p$K_a$) at the interface has to be envisaged. It can be estimated as:

$$K_a^{int} = \frac{[O_2^-][H^+]}{[HO_2]} = K_a^{bulk} e^{-\delta\Delta G_{eq}/RT} \quad (4)$$

where $\delta\Delta G_{eq}$ represents the whole energy change for the equilibrium in the interface or the bulk. If we assume the energies reported above for the hydroxyperoxide and superoxide radicals, $\delta\Delta G \approx 2$ kcal mol$^{-1}$, an effective increase of the p$K_a$ at the interface by 1–2 units is predicted. Consequently, an attenuation of the role of ionic mechanisms involving $O_2^-$ on the overall interfacial processes upon $HO_2$ adsorption on the droplet is expected.

Further interface solvation effects on the chemical properties of these radicals can be analyzed by looking at the energy variation of the highest (singly) occupied and lowest unoccupied molecular orbitals, HOMO and LUMO. Figure 5 displays the corresponding average values as a function of the distance with respect to the interface (1000 snapshots were used per point from the umbrella sampling calculations). For comparison, properties computed in the gas

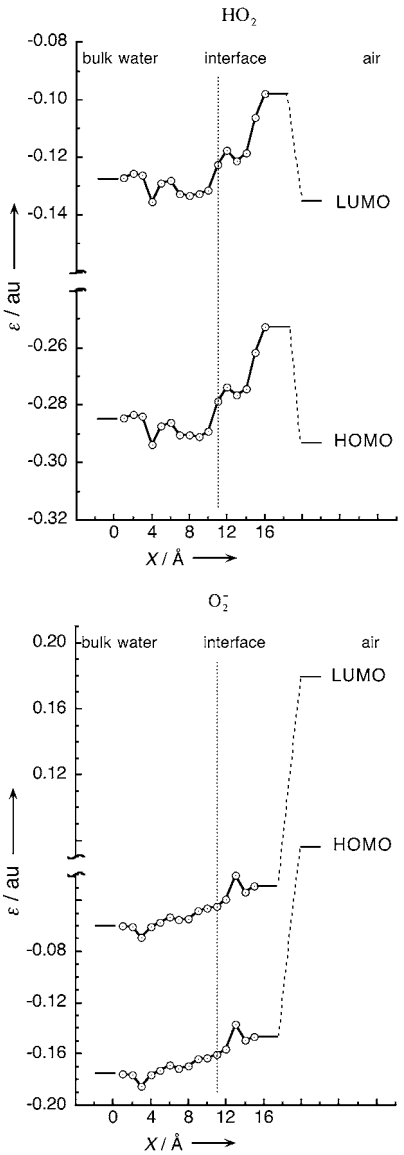


***Figure 5.*** HOMO and LUMO energies of the studied radicals in the gas phase, at the water–air interface, and in bulk water. Averages were obtained using the B3LYP/aug-cc-pVTZ level of calculation and snapshots from the umbrella sampling QM/MM simulations. $X = 0$ corresponds to the center of the simulation box.

phase are also shown (B3LYP/aug-cc-pVTZ calculations using optimized geometries at the B3LYP/6-311 + G* level). For $O_2^-$, the uptake process produces a huge decrease of the HOMO and LUMO frontier orbital energies, as expected from simple considerations of ion solvation. A largest part of the energy drop is reached when the anion approaches the water surface but as the anion moves into the bulk, further stabilization is achieved. Remarkably, in the case of the $HO_2$ radical, the HOMO and LUMO energies exhibit a net maximum when the system is close to the interface, with significant differences with respect to either gas phase or bulk solution. This finding is rather surprising, because in principle the interface properties would be expected to be intermediate between those of the two phases, as predicted for the

  

superoxide anion. It can be explained however by taking into account the nature of the solute–solvent interactions at the interface, where $HO_2$ behaves essentially as a proton donor (Figure 4). It has been shown[18] that H-bonds with water may produce either a destabilization (proton donor) or a stabilization (proton acceptor) of the $H_2O_2$ frontier orbitals, and a similar behavior is expected for $HO_2$. It should be noted however that other electronic properties do not follow the same trend as the orbital energies. For example, the $HO_2$ dipole moment at the interface (3.05 D) is intermediate between that in gas phase (2.21 D) and bulk solution (3.35 D). The interfacial solvation effects on the HOMO and LUMO energies are expected to produce significant changes in terms of electron donor–acceptor capability of the radicals. In particular, the electron transfer from $O_2^-$ to $HO_2$ [Eq. (3)] might require lower activation energy because the corresponding HOMO ($O_2^-$)–LUMO ($HO_2$) gap decreases from bulk water to the interface by roughly 0.02–0.03 au (0.5–0.8 eV).

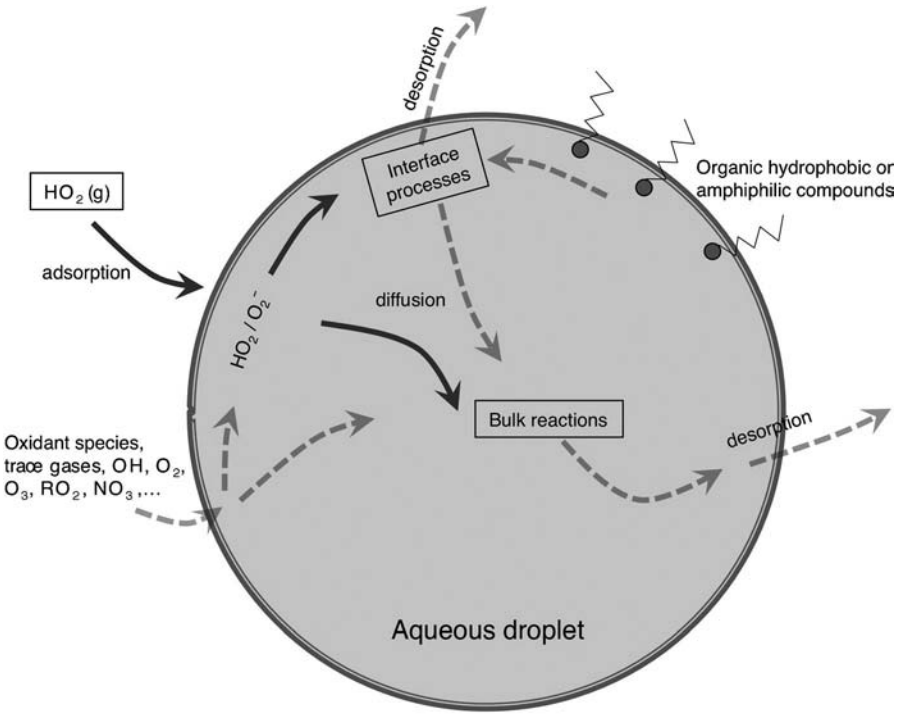


***Figure 6.*** Representation of $HO_2$ reactions after adsorption onto a water droplet.

Similarly, the redox potential of the $O_2/O_2^-$ couple would be modified and so would be the reactivity with oxidant compounds present in the medium. The order of magnitude can be obtained using the interface/bulk differences in solvation energies for the reduced form $O_2^-$ ($\delta\Delta G_{solv} \approx +5\ kcal\,mol^{-1}$, see above) and the oxidized one $O_2$. The solvation process of the dioxygen molecule was not studied here, but an estimation has been made in the work of Vácha et al. using classical MD simulations.[3a] This (hydrophobic) molecule exhibited a net free energy minimum at the interface with a differential solvation energy $\delta\Delta G_{solv} \approx -2.5\ kcal\,mol^{-1}$ (the experimental bulk free energy of solvation is $+4\ kcal\,mol^{-1}$ [9]). Using these quantities, it becomes possible to evaluate the interface redox potential of the couple, or more precisely, the difference with respect to bulk properties. A redox potential decrease of $-0.32$ V was obtained, which is as large as the experimental redox potential in bulk water ($-0.33$ V).[19] Thus, the superoxide anion formed by dissociation of $HO_2$ would have an enhanced reactivity at the air–water interface that will favor Reaction (3) but also reactions with oxidant species residing preferentially at the interface, such as hydrophobic or amphiphilic organic compounds.

In summary, chemistry at the air–water interface with $HO_2$ is found to be different from bulk and also different from the gas phase. This has significant ramifications for $HO_2$ chemistry or aerosol and cloud chemistry (Figure 6). At the interface, two main effects influencing the reactivity can be expected: a) A decrease of ionic dissociation constant by about 1–2 units and increase of $HO_2$ concentration with respect to the bulk; and 2) a change of the $O_2/O_2^-$ redox potential by about $-0.3$ V.

## Experimental Section

Combined QM/MM simulations were carried out at $T = 298$ K using a Nosé–Hoover thermostat.[20] The box size is [Å] is $24.662 \times 24.662 \times 130$. In the umbrella sampling calculations of the potential of mean force, the reaction coordinate is taken as the distance between the center of mass of the solute and the center of mass of the solvent. This distance was varied by steps of 0.25 Å and the bias potential force constant is $k = 10\ kcal\,mol^{-1}\,Å^2$. After thermalization, the trajectory was carried out for 10 ps at each point of the reaction coordinate. Unconstrained trajectories of 50 ps were also carried out with the solute initially placed at the air–water interface.

Received: January 23, 2012
Revised: February 20, 2012
Published online: March 21, 2012

**Keywords:** atmospheric chemistry · hydroperoxide · molecular dynamics · superoxide · water droplets

[1] M. O. Andreae, P. J. Crutzen, *Science* **1997**, *276*, 1052–1058.
[2] D. J. Jacob, *Atmos. Environ.* **2000**, *34*, 2131–2159.
[3] a) R. Vácha, P. Slavíček, M. Mucha, B. J. Finlayson-Pitts, P. Jungwirth, *J. Phys. Chem. A* **2004**, *108*, 11573–11579; b) S. D. Belair, H. Hernandez, J. S. Francisco, *J. Am. Chem. Soc.* **2004**, *126*, 3024–3025; c) M. Torrent-Sucarrat, M. F. Ruiz-Lopez, M. Martins-Costa, J. S. Francisco, J. M. Anglada, *Chem. Eur. J.* **2011**, *17*, 5076–5085; d) Q. Shi, S. D. Belair, J. S. Francisco, S. Kais,

  

*Proc. Natl. Acad. Sci. USA* **2003**, *100*, 9686 – 9690; e) A. Morita, Y. Kanaya, J. S. Francisco, *J. Geophys. Res. D* **2004**, *109*, 09201 – 09210.
[4] a) I. Tuñón, M. T. C. Martins-Costa, C. Millot, M. F. Ruiz-Lopez, *Chem. Phys. Lett.* **1995**, *241*, 450 – 456; b) M. Strnad, M. T. C. Martins-Costa, C. Millot, I. Tuñón, M. F. Ruiz-López, J. L. Rivail, *J. Chem. Phys.* **1997**, *106*, 3643 – 3657; c) S. Chalmet, M. F. Ruiz-López, *J. Chem. Phys.* **2006**, *124*, 194502; d) M. T. C. Martins-Costa, M. F. Ruiz-López, *Chem. Phys.* **2007**, *332*, 341 – 347.
[5] W. L. Jorgensen, J. Chandrashekar, J. D. Madura, W. R. Impey, M. L. Klein, *J. Chem. Phys.* **1983**, *79*, 926 – 935.
[6] A. D. Becke, *J. Chem. Phys.* **1993**, *98*, 5648 – 5652.
[7] G. M. Torrie, J. P. Valleau, *J. Comput. Phys.* **1977**, *23*, 187 – 199.
[8] a) S. Kumar, J. M. Rosenberg, D. Bouzida, R. H. Swendsen, P. A. Kollman, *J. Comput. Chem.* **1992**, *13*, 1011 – 1021; b) B. Roux, *Comput. Phys. Commun.* **1995**, *91*, 275 – 282.
[9] R. Sander, in Compilation of Henry's Law Constants for Inorganic and Organic Species of Potential Importance in Environmental Chemistry (Version 3), Vol. http://www.mpchmainz.mpg.de/~sander/res/henry.html, **1999**.
[10] R. G. Pearson, *J. Am. Chem. Soc.* **1986**, *108*, 6109 – 6114.
[11] X. Yang, B. Kiran, X. B. Wang, L. S. Wang, M. Mucha, P. Jungwirth, *J. Phys. Chem. A* **2004**, *108*, 7820 – 7826.
[12] J. Li, H. Hou, B. Wang, *J. Phys. Chem. A* **2009**, *113*, 800 – 804.
[13] J. Shen, C. F. Wong, J. A. McCammon, *J. Comput. Chem.* **1990**, *11*, 1003 – 1008.
[14] P. A. Narayana, D. Suryanarayana, L. Kevan, *J. Am. Chem. Soc.* **1982**, *104*, 3552 – 3555.
[15] M. K. Petersen, S. S. Iyengar, T. J. F. Day, G. A. Voth, *J. Phys. Chem. B* **2004**, *108*, 14804 – 14806.
[16] a) P. B. Petersen, R. J. Saykally, *J. Phys. Chem. B* **2005**, *109*, 7976 – 7980; b) T. L. Tarbuck, S. T. Ota, G. L. Richmond, *J. Am. Chem. Soc.* **2006**, *128*, 14519 – 14527; c) S. Iuchi, H. N. Chen, F. Paesani, G. A. Voth, *J. Phys. Chem. B* **2009**, *113*, 4017 – 4030; d) H. Takahashi, K. Maruyama, Y. Karino, A. Morita, M. Nakano, P. Jungwirth, N. Matubayasi, *J. Phys. Chem. B* **2011**, *115*, 4745 – 4751.
[17] a) V. Buch, A. Milet, R. Vácha, P. Jungwirth, J. P. Devlin, *Proc. Natl. Acad. Sci. USA* **2007**, *104*, 7342 – 7347; b) J. K. Beattie, A. M. Djerdjev, G. G. Warr, *Faraday Discuss.* **2008**, *141*, 31 – 39; c) P. B. Petersen, R. J. Saykally, *Chem. Phys. Lett.* **2008**, *458*, 255 – 261; d) B. Winter, M. Faubel, R. Vácha, P. Jungwirth, *Chem. Phys. Lett.* **2009**, *474*, 241 – 247; e) C. J. Mundy, I. F. W. Kuo, M. E. Tuckerman, H. S. Lee, D. J. Tobias, *Chem. Phys. Lett.* **2009**, *481*, 2 – 8.
[18] Ref. [4d].
[19] P. M. Wood, *FEBS Lett.* **1974**, *44*, 22 – 24.
[20] a) S. Nosé, *J. Chem. Phys.* **1984**, *81*, 511 – 519; b) W. G. Hoover, *Phys. Rev. A* **1985**, *31*, 1695 – 1697.

  